Wind and Structures, *Vol. 24, No. 2 (2017) 95-118*
DOI: https://doi.org/10.12989/was.2017.24.2.095

Effect of internal angles between limbs of cross plan shaped tall building under wind load

Debasish Kumar[a] and Sujit Kumar Dalui[*]

Civil Engineering Department, Indian Institute of Engineering Science and Technology, Shibpur, Howrah-711103, India

(Received August 12, 2016, Revised November 17, 2016, Accepted November 26, 2016)

Abstract. The present study revealed comparison the pressure distribution on the surfaces of regular cross plan shaped building with angular cross plan shaped building which is being transformed from basic cross plan shaped building through the variation of internal angles between limbs by 15^o for various wind incidence angle from 0^o to 180^o at an interval of 30^o. In order to maintain the area same the limbs sizes are slightly increased accordingly. Numerical analysis has been carried out to generate similar nature of flow condition as per IS: 875 (Part –III):1987 (a mean wind velocity of 10 m/s) by using computational fluid dynamics (CFD) with help of ANSYS CFX (k-ε model). The variation of mean pressure coefficients, pressure distribution over the surface, flow pattern and force coefficient are evaluated for each cases and represented graphically to understand extent of nonconformities due to such angular modifications in plan. Finally regular cross shaped building results are compared with wind tunnel results obtained from similar '+' shaped building study with similar flow condition. Reduction in along wind force coefficients for angular crossed shaped building, observed for various skew angles leads to develop lesser along wind force on building compared to regular crossed shaped building and square plan shaped building. Interference effect within the internal faces are observed in particular faces of building for both cases, considerably. Significant deviation is noticed in wind induced responses for angular cross building compared to regular cross shaped building for different direction wind flow.

Keywords: CFD; wind incidence angle; cross plan shaped building; k-ε turbulence model; pressure co-efficient and force coefficient

1. Introduction

With the development in the construction technology over last few decades and scarcity of accessible land in the important cities demand for high-rise buildings and skyscrapers are increasing day by day. These high-rise buildings stand as a landmark of the locality and needed to be architecturally unique and attractive, lead to be complex in geometric shape in plan as well as in elevation. Indian code of practices for wind load estimation [i.e., IS:875(Part-III):1987] unable to predict the wind induced design parameter of building of such complex geometric plan shaped building like '+', 'U','V', 'L', 'E','Y' plan shaped buildings or a combination of these shapes,

∗Corresponding author, Assistant Professor, E-mail: sujit.dalui@gmail.com
[a] Ph.D. Student, Email: debasishkumar0@gmail.com

http://www.techno-press.org/?journal=was&subpage=8 ISSN: 1226-6116 (Print), 1598-6225 (Online)

encourage the researchers to enlighten in this dark areas. Lam, Wong *et al*. (2009) investigated the size effects of recessed cavity on dynamic wind load behaviour with varying wind incidence angle for 'H' plan shaped building**.**

Amin and Ahuja (2013) predicted the effects of side ratio on rectangular plan shaped building experimentally. Kushal, Ahuja *et al.* (2013) experimentally evaluated the variation of pressure coefficients on different faces of 'T' plan shaped building. Verma, Ahuja *et al.* (2013) described the effects of the wind incidence angle on pressure distribution on square plan shaped building. In the year 2014, Bhattacharyya, Dalui *et al.* (2014) carried out the detailed numerical and experimental studies on variation of wind pressure on 'E' plan shaped building with various wind incidence angle. Comparative study of peculiarity on surface pressures distribution on '+' plan shaped building by using both wind tunnel study and numerical study for limited 0^o and 45^o wind incidence angles have been carried out by Chakraborty, Dalui *et al*. (2014a,b). Mukherjee, Chakraborty *et al.* (2014) carried out experimental and numerical comparative studies of the pressure developed on the different faces of 'Y' plan shaped building for specific skew angles (0^o, 60^o and 90^o). Numerical study was carried out using computational fluid dynamics package of ANSYS CFX using turbulence model of 'k-ε' and shear stress transport (SST) model. Tanaka *et al.* (2012) conducted an extensive experimental studies of the different aerodynamic modifications for wind resistant of tall building to effectively reducing the aerodynamic forces and wind pressures for various skew angles. Gu (2009) introduced the concept of 'mode coupling factor' and modified SRSS method for evaluation of wind response and equivalent static wind load for tall building and structure through a series of wind tunnel studies by wind pressure and scanning HFFB techniques. Amin and Ahuja (2012) enumerated the interference effects of two closely placed buildings with 'L' and 'T' plan shaped for various wind incidence angle. Raj and Ahuja (2013) experimentally investigated the variation of force coefficients and moment coefficients for building with different limbs dimensions with various flow directions.

Computational Fluid Dynamics (CFD) plays an important role to numerically simulate similar environmental condition around the building and the entire information prevailing to the wind-structure interaction can be evaluated. Thus CFD has been used rapidly since last few decades. Many researchers like Sevalia, Desai *et al.* (2012) supersede the use of wind tunnel studies with CFD to explore force coefficient for different plan shaped building circular, square, '+', hexagonal and octagonal plan shaped building model. Gomes, Rodrigues *et al.* (2005) compared surface pressure distributions using the experimental and Computational Fluid Dynamics (CFD) analysis on 'L' and 'U' plan shaped with respect to regular square plan shaped building. Juretic and Kozmar (2013) carried out a novel approach of using k-ε model, focusing on Reynolds stresses in computational simulation of atmospheric boundary layer flow, capable of simulating reduction of turbulence intensity with height. Good agreement of mean velocity, turbulence kinetic energy and Reynolds stress profile observed between experimental and computational method using k-ε method. Dagnew, Bitsuamalk *et al.* (2009) used k-ε RANS and LES model to numerically find out wind pressure variation and interference effects of rectangular building with respect to CAARC (Commonwealth Advisory Aeronautical Council) standard tall building model. Fu, Li *et al.* (2008) related the field measurement data and wind tunnel test data for two super tall buildings on similar boundary layer wind characteristic over typical open country and urban terrain and the results showed a good agreement (variations are within 20-25%) between them. Mendis, Ngo *et al.* (2007) overviewed that wind induced responses like along wind and across wind effects etc. and interference effects on building surfaces can be evaluated accurately both using wind tunnel test and Computational Fluid Dynamic (CFD) analysis

without much discrepancies (within reliable range of 20-25%) in results. Braun and Agerneh (2009) conferred that satisfactory converging relation between wind tunnel test and numerical analysis are revealed in evaluating pressure and aerodynamic coefficients of tall building over CAARC (Commonwealth Advisory Aeronautical Council) standard building model. Zhou, Kijewski *et al.* (2002) suggested the variation of definition of wind flow characteristic plays the pivotal role for scattering of wind load calculations for tall buildings of different international wind codes of practices.

Interference effect on wind induced responses are very important aspect now-a-day, should be taken into account for tall and high rise building. The close proximity of surrounding building around the principal building, may produce shielding effect but depending upon the position and height of building and other important factors it may causes vulnerable effects too. Many researchers are working on the interference effect on structures. Recently, Bairagi and Dalui (2014), evaluated optimum position of two high-rise rectangular buildings in different orientation and also for different wind incidence angle based on interference factor (IF) calculations numerically. Kheyari and Dalui (2014), using ANSYS CFX package numerically studied the variation of pressure coefficients on the faces of principal rectangular building due to presence of upstream building with varying height aspect ratio from 1:5 to 5:5 for different skew angles. Further, optimum spacing between upstream and principal building are evaluated to avoid interference effect for along wind and across wind direction. Interference effect due to presence of more than two buildings are studied by Kar *and Dalui* (2015), carried out using ANSYS CFX package with k-ε turbulence model to numerically evaluate the variation pressure on different faces of octagonal building surrounded by the three square plan shaped building at different orientation and finally expressed the in terms of interference factor (IF) comparing the results with similar isolated octagonal building.

2. Scope of work

This paper mainly focused on the variation of pressure coefficients on the surfaces of building and force coefficients on whole building for cross plan shaped building (i.e., regular cross plan shaped building (Type-I)) having internal angles (α_1,α_2) between each limbs are 90^o each (Figs. 1 and 2). Further keeping the plan area same internal angle between limbs (α_1,α_2) are changed by 15^o leads to transformed into angular cross plan shaped building (Type-II) shown in the Figs. 3 and 4. But total angle between each limbs i.e., $\alpha_1+\alpha_2 = 180^o$ should be satisfied at both cases. For both cases wind incidence angles are varying from 0^o to 180^o at an interval of 30^o.

The each limb dimension of the Type-I building model are 100 mm in length and 50 mm width and overall height of the building is 500 mm (Fig. 2). The total plan area of model is 22500 mm^2. To keep plan area remains same, length of model for Type –II building is required to be increased marginally for Type- II building. Details dimension of the plan for Type-II building is shown in Fig. 4. Both models are used to comprehend the wind induced responses on different faces of building for various skew angle of wind flow ranging from 0^o to 180^o at in interval of 30^o.

3. Numerical study

Numerical simulations were carried out in this study through Computational Fluid Dynamics

(CFD) package ANSYS 14.5. There are several turbulence models available for simulation. Among the models, k-ε and Shear Stress Transport (SST) model are widely used in literature. The SST models can predicts responses more accurately in high turbulence zone while the k-ε model is better for overall moderate turbulence as concluded by Chakraborty, Dalui *et al.* (2014a, b).Therefore, here k-ε turbulence model is used to assess the wind-structure interaction characteristic. A comparative study of k-ε model with SST model has been conducted and presented in the section 4.6.

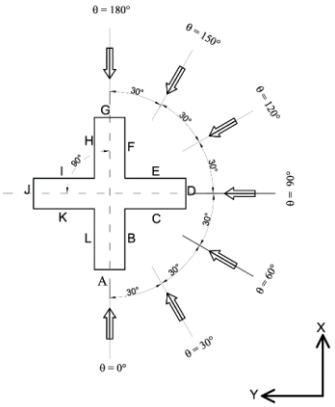

Fig. 1 Variation of angle of attack on regular plan shaped building with face notation

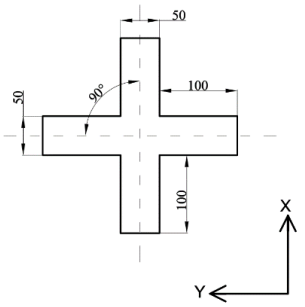

Fig. 2 Dimension of regular plan shaped building in plan

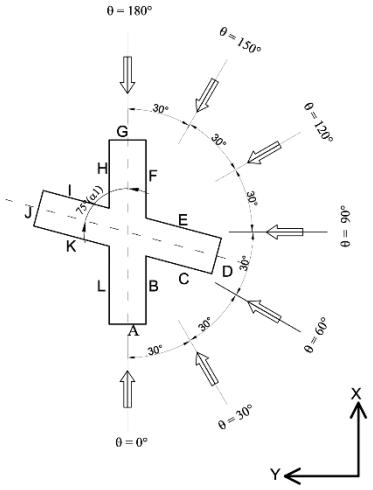

Fig. 3 Variation of angle of attack on angular plan shaped building with face notation

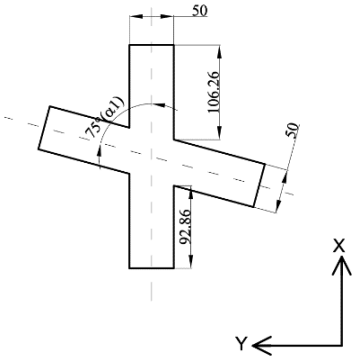

Fig. 4 Dimension of angular plan shaped building in plan

Gradient diffusion hypothesis used in k-ε model to relate the Reynolds stresses to the mean velocity gradients and turbulence viscosity. '*k*' is the turbulence kinetic energy defined as the variance of fluctuations in velocity and 'ε' is the turbulence eddies dissipation (the rate at which the velocity fluctuation dissipates). Therefore, continuity and momentum equations modified to Eqs. (1)-(7) as given below

$$\frac{\partial \rho}{\partial t} + \frac{\partial}{\partial x_j}\left(\rho U_j\right) = 0 \tag{1}$$

$$\frac{\partial \rho U_i}{\partial t} + \frac{\partial}{\partial x_j}(\rho U_i U_j) = \frac{\partial P'}{\partial x_i} + \frac{\partial}{\partial x_j}\left[\mu_{eff}\left(\frac{\partial U_i}{\partial x_j} + \frac{\partial U_j}{\partial x_i}\right)\right] + S_M \tag{2}$$

Where, S_M is equal to the sum of the body forces, μ_{eff} is the effective viscosity accounting for turbulence and p' is the modified pressure. This k-ε model, similar to the zero equation model, is based on the eddy viscosity concept. So that,

$$\mu_{eff} = \mu + \mu_t \tag{3}$$

Where, μ_t is the turbulence viscosity .The k-ε model assumes that turbulence viscosity is linked to the turbulence kinetic energy and dissipation via the relation.

$$\mu_t = C_\mu \rho \frac{k^2}{\varepsilon} \tag{4}$$

Where, C_μ is a constant with a value of 0.09. The values of k and ε come directly from the differential transport equations for the turbulence kinetic energy and turbulence dissipation rate.

$$\frac{\partial(\rho k)}{\partial t} + \frac{\partial}{\partial x_j}(\rho U_j k) = \frac{\partial}{\partial x_j}\left[\left(\mu + \frac{\mu_t}{\sigma_k}\right)\frac{\partial k}{\partial x_j}\right] + P_k - \rho\varepsilon + P_{kb} \tag{5}$$

$$\frac{\partial(\rho \varepsilon)}{\partial t} + \frac{\partial}{\partial x_j}(\rho U_j \varepsilon) = \frac{\partial}{\partial x_j}\left[\left(\mu + \frac{\mu_t}{\sigma_\varepsilon}\right)\frac{\partial \varepsilon}{\partial x_j}\right] + \frac{\varepsilon}{k}(C_{\varepsilon 1} P_k - C_{\varepsilon 2}\rho\varepsilon + C_{\varepsilon 1} P_{\varepsilon b}) \tag{6}$$

P_k is the turbulence production due to viscous forces, which is modelled using

$$P_k = \mu_t\left(\frac{\partial U_i}{\partial x_j} + \frac{\partial U_j}{\partial x_i}\right)\frac{\partial U_i}{\partial x_j} - \frac{2}{3}\frac{\partial U_k}{\partial x_k}\left(3\mu_t \frac{\partial U_k}{\partial x_k} + \rho k\right) \tag{7}$$

$C_{\varepsilon 1}$ and $C_{\varepsilon 2}$ are also k-ε turbulence model constants in ANSYS CFX values are 1.44 and 1.92 respectively. σ_k is the turbulence model constant for k equation with a value of 1.0 and σ_ε is also a turbulence model constant with a value of 1.30. ρ is taken as 1.224 kg/m^3 as density of air. μ_t is turbulence viscosity. The buildings are considered as bluff body and flow pattern around the building is studied.

3.1 Domain size, model details and mesh details

Domain size shall be chosen so the vortex generations in the wake region, velocity fluctuation etc. can be effectively incorporated. According to Revuz, Hargreaves *et al*. (2012) upstream, downstream, two side clearances and top clearance are 5H, 15H, 5H and 5H respectively from the extreme edges of object building as shown in Fig. 5. Where, H is the height building model being considered. The scale of building model is 1:300 and velocity scale is 1:5. The limb dimension

of the Type-I building model are 100 mm in length, 50 mm width and 500 mm height as discussed earlier. The mean inlet velocity considered is to be 10 m/s with turbulence intensity in the range of 5 % -10% to simulate similar nature of boundary layer wind flow for terrain category -2 as per IS:875(Part –III):1987 prevailing around the building. To generate velocity profile of atmospheric boundary layer flow power law is used as shown in Eq. (8).

$$\frac{U}{U_o} = \left(\frac{z}{z_o}\right)^{\alpha} \tag{8}$$

Where, U_o is the basic wind speed taken as 10 m/s.
Z_o is boundary layer height scaled down to 1 m.
α is power index is taken as 0.133.

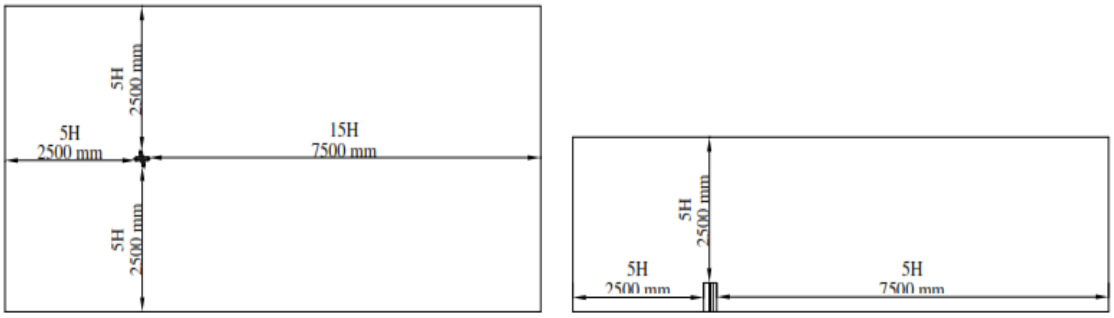

(a) Plan (b) Elevation

Fig. 5 Plan and elevation of domain and building.

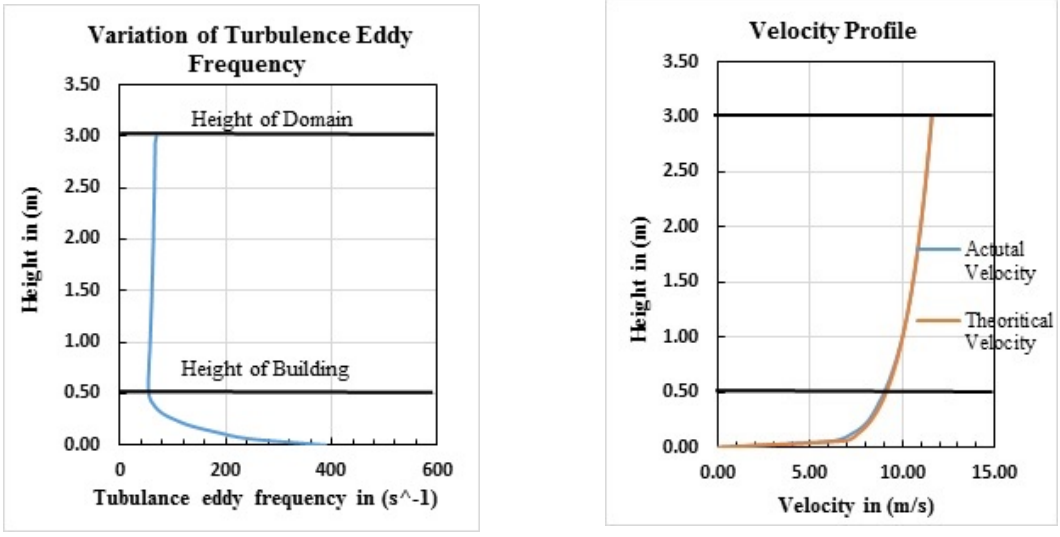

(a) (b)

Fig. 6 (a) Variation of turbulence eddy frequency with height of building and (b) Variation of velocity with the height of building.

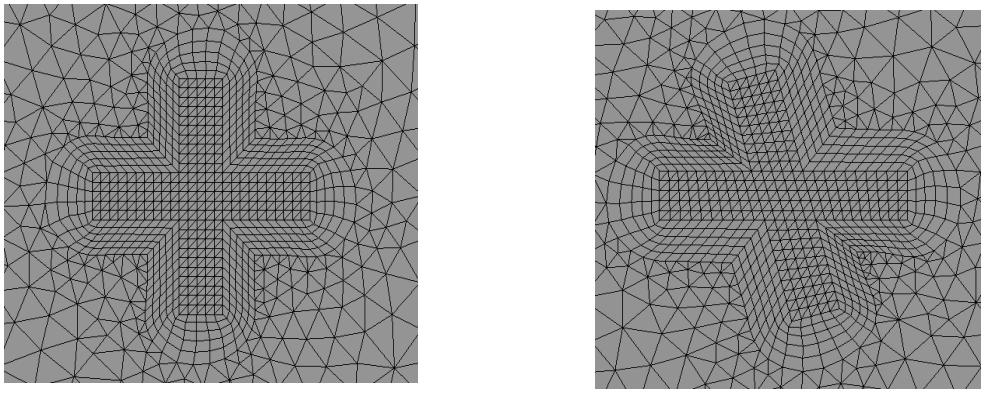

(a) (b)

Fig. 7 (a) Typical mesh detail surrounding building for Type–I and (b) Typical mesh detail surrounding building for Type–II.

The velocity profile and turbulence eddy frequency profile along the height of the domain are plotted in the Figs. 6(a) and 6(b). The velocity in other directions and relative pressure are considered as nil respectively. In order to get pressure contour, the building surfaces shall be considered as no slip condition whereas side faces and top surface of the domain the considered to be as free slip wall. A combination of tetrahedron and hexagonal meshing shall be considered for meshing the domain and surfaces of building models as shown in Figs. 7(a) and 7(b). Finer meshing near and on the surfaces of building leads to simulate uniform flow and accurately assess the actual response of the building faces. While uniform coarser meshing in the rest of the domain is considerably reduced the time of analysis without significant loss of accuracy.

3.2 Validation

The validity of ANSYS CFX package for numerical simulation should be checked before finally use for respective models of present study. Thus one square plan shaped building taken into consideration having dimension of 100 mm X 100 mm [width (a) x length (b)] with height (h) of 500 mm [Figs. 8(a) and 8(b)] The velocity at inlet is 10m/s and side clearances from the building faces is accordance to Revez, Hargreaves *et al.* (2012) (Fig. 5). The turbulence intensity is corresponding to 5%-10%. The mean pressure coefficients and force coefficients of building surfaces are tabulated and detailed comparative study is made with the obtained values using numerical results with various international standards.

The mean pressure coefficients using ANSYS CFX are in good agreement with AS/NZS 1170.2:2002 and also within tolerance limit with other international standards (Table 1). The calculated force coefficients values almost matched with ASCE 7-10 and also within acceptable limit with other international standards (Table 2). The main difference in the basic values are due to different technique and different metrological data are considered for evaluation. From the comparative statement it can be concluded that ANSYS CFX can be used as numerical simulation of structure.

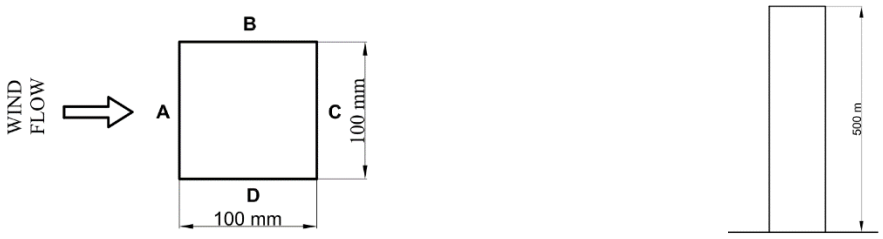

Fig. 8 (a) Plan of square plan shaped building and (b) Elevation of square plan shaped building

Table 1 Comparison of mean pressure coefficient (Cp) between different International Standards and ANSYS CFX

Standards / Face	ANSYS CFX	AS/NZS-1 170.2 (2002)	Deviation w.r.t. AS/NZS-11 70.2 (2002)	ASCE 7-10	Deviation w.r.t. ASCE 7 -10	IS :875(Part –III) :1987	Deviation w.r.t. IS :875(Part – III) :1987
Face A	(+) 0.80	(+) 0.80	0%	(+)0.80	0%	(+)0.80	0%
Face B	(-) 0.60	(-) 0.65	7.7% dec	(-) 0.70	14.3% dec	(-) 0.80	25% dec
Face C	(-) 0.50	(-) 0.50	0%	(-) 0.50	0%	(-) 0.25	100% inc
Face D	(-) 0.60	(-) 0.65	7.7% dec	(-) 0.70	14.3% dec	(-) 0.80	25% dec

(+) : pressure ; (-) : suction; dec : decrease ; inc: increase

Table 2 Comparison of force coefficient (C_f) between different International Standards and ANSYS CFX

Standards / Face	ANSYS CFX	ASCE 7-10	Deviation w.r.t. ASCE 7-10	IS :875(Part –III) :1987	Deviation w.r.t. IS :875(Part –III) :1987	AS/NZS-1 170.2 (2002)	Deviation w.r.t. AS/NZS 1170.2 (2002)
a/b = plan ratio	1	any	any	1	1	1	1
h/b=aspect ratio	5	1< h/b ≤7	1< h/b ≤7	5	5	any	any
Force coefficient (C_f)	1.408	1.40	0.5% inc	1.350	4.30% inc	(+) 2.2	36.0% dec

dec : decrease ; inc: increase

4. Results and discussion

4.1 Flow pattern

Fig. 9(a) presents the flow generated around the building for regular cross shaped building for 0^o wind incidence angle. The generated vortices are symmetrical in nature in wake region of the building. High separation of flow are observed on side faces like face D and face J, resulting high suction near the face edges. Flow pattern of angular cross shaped building is more or less symmetrical for 0^o wind angle having larger eddies are observed on one side as shown in Fig. 9(b).

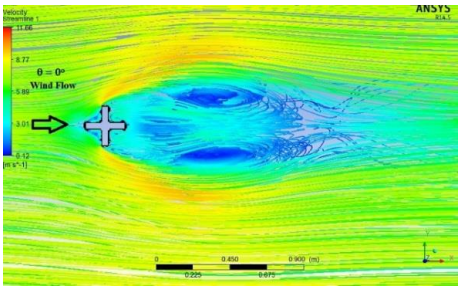

(a)

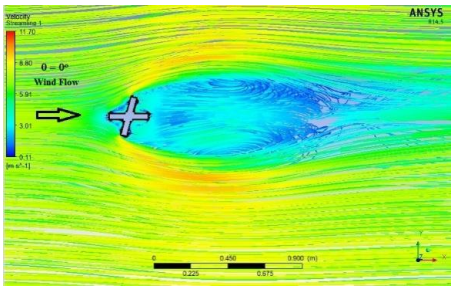

(b)

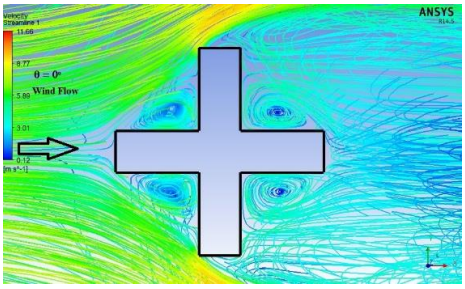

(c)

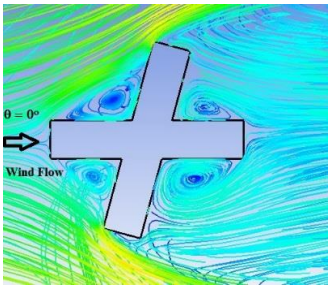

(d)

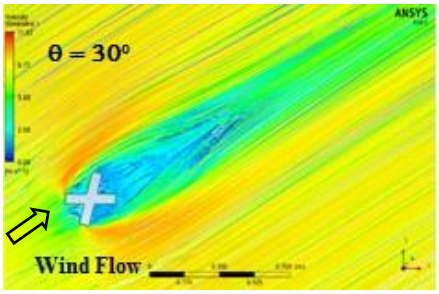

(e)

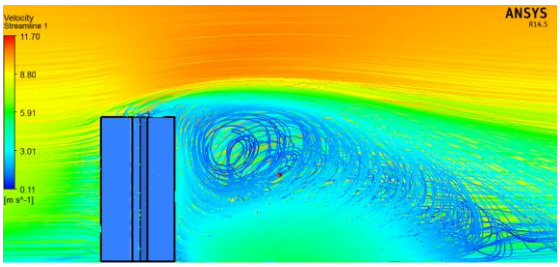

(f)

Fig. 9 (a) Variation of flow for TYPE –I building for 0^o angle of attack, (b) Variation of flow for TYPE –II building for 0^o angle of attack, (c) Closer view flow pattern around the Type –I building for 0^o wind angle, (d) Closer view flow pattern around the Type –II building for 0^o angle of attack, (e) Flow pattern for Type –II building for 30^o angle of attack and (f) Flow pattern around the building for Type-II Building –side elevation

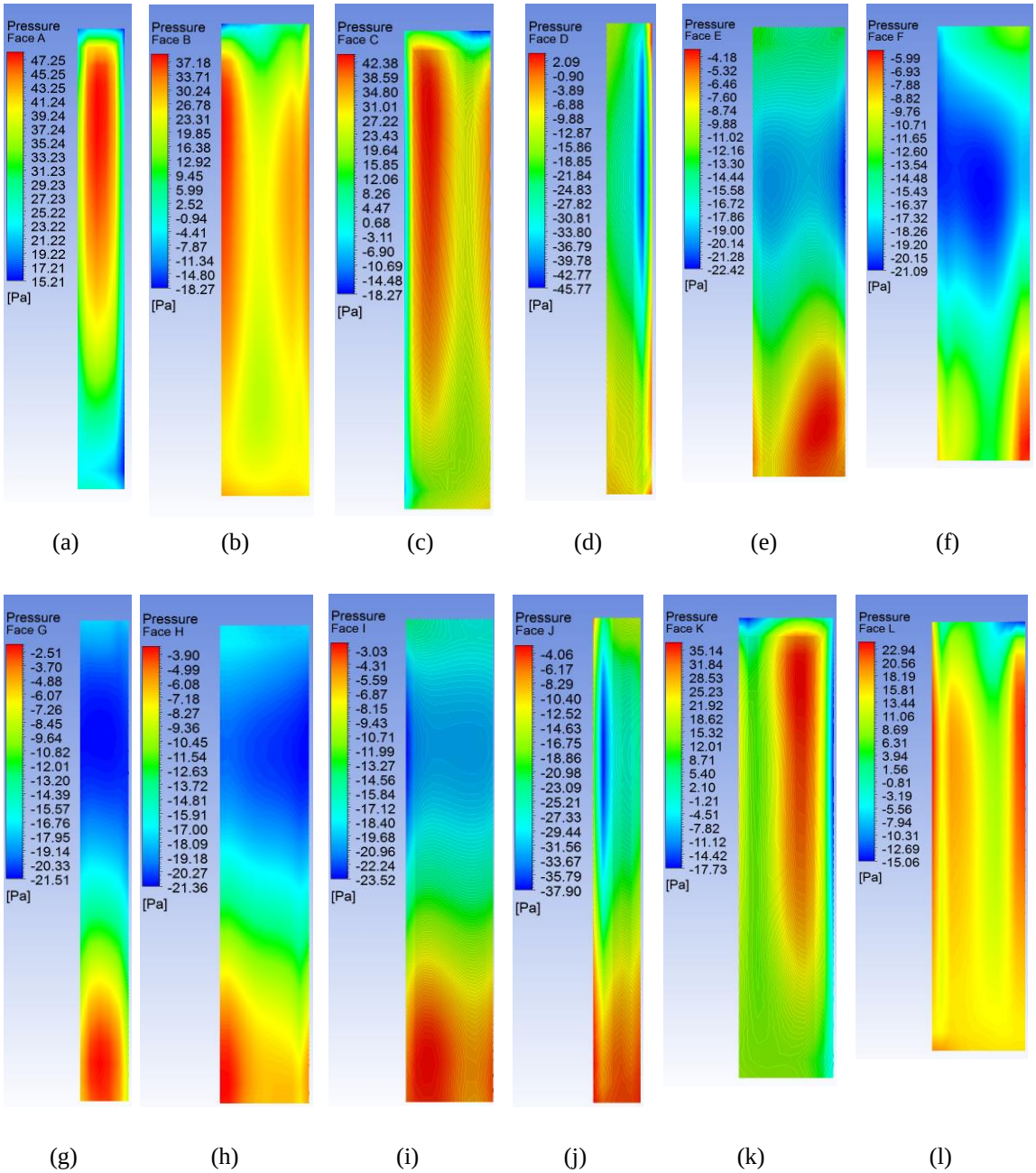

(a) (b) (c) (d) (e) (f)

(g) (h) (i) (j) (k) (l)

Fig. 10 Pressure contour for 0^{o} wind incidence angle for angular cross shaped building (Type – II) (a) Face A, (b) Face B, (c) Face C, (d) Face D, (e) Face E, (f) Face F, (g) Face G, (h) Face H, (i) Face I, (j) Face J, (k) Face K and (l) Face L

A closer observation reveals the evidence of interference effects within the internal faces of building for both Type I and Type-II building (like, for side faces of frontal limb on windward side, face B and face L) shown in Figs. 9(c) and 9(d). The flow pattern for 30^o skew angle for type II building is also shown in Fig. 9(e) and further prominent vortex shedding has been noticed on the back side of building and top the building for Type II building for 0^o wind angle (Fig. 9(f)). Streamline of flow are closer to each other due to separation of flow above and side of the building, resulting an increase in velocity.

4.2 Pressure distribution

The pressure contour of different faces of angular cross building model for 0^o angle of attack are shown in the Figs. 10(a)-10(l). Face A experienced positive pressure with maximum around three quarter height from base and the flow pattern is not symmetrical about vertical axis, slightly shifted towards face B. Major portion of the face B and face C are subjected to positive pressure while only few portion around the top experienced negative pressure i.e., suction. Due to large flow separation, side face D experienced significant suction with higher value around the edge. Moderate suction are observed on face E and face F, almost similar in nature. Due to leeward position for 0^o wind incidence angle, face G, face H and face I are subjected to suction and maximum around the mid height of building. Relatively higher suction is noticed on face J, particularly near the edge of connecting side faces due to separation of wind flow. However face K is directly exposed to windward flow positive pressure should be perceived throughout face but prominent suction is noticed near the edges owing to interference effect from face L, reversing the direction of flow. Major portion of face L is experienced with positive pressure except top corner.

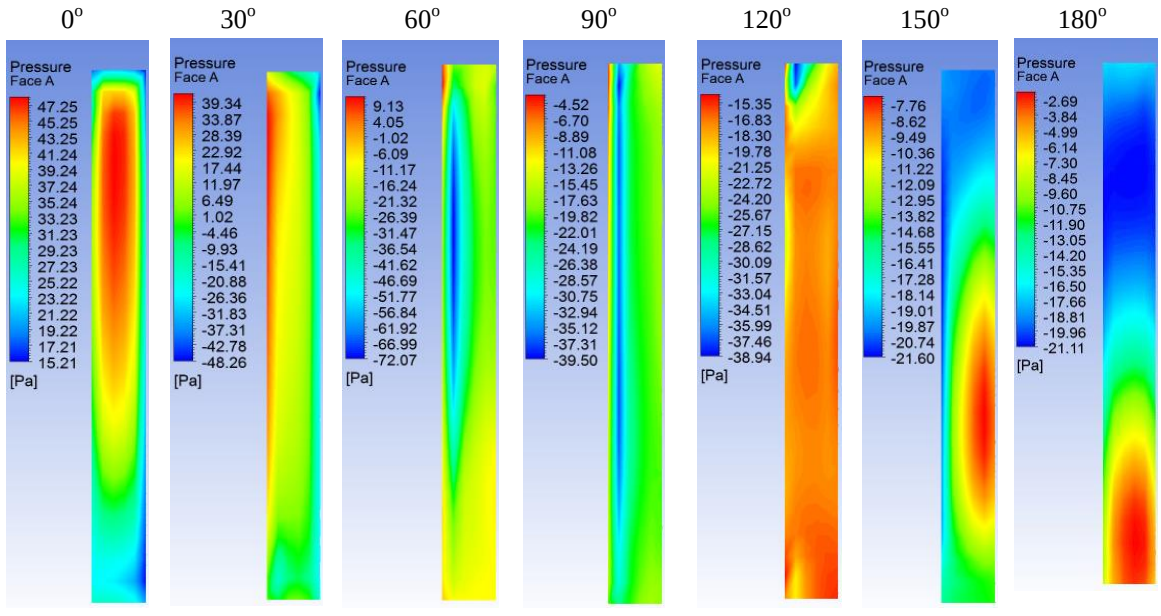

Fig. 11 Pressure contour of face A of building for various wind incidence angle for angular cross shaped building (Type – II) (a) 0^o, (b) 30^o , (c) 60^o , (d) 90^o , (e) 120^o , (f) 150^o and (g) 180^o

Figs. 11(a)-11(g) are representing the variation of pressure contour on face A for different skew angle from 0^o to 180^o at an interval of 30^o. Maximum positive pressure is observed for 0^o angle of attack near the ¾ th of overall depth of building from base. For 30^o wind incidence angle, lesser positive pressure is experienced near the edge of face B but extreme top portion is subjected to very high suction. Due to large separation of wind flow near edges of face B huge suction is noticed at mid height of building for 60 ^{o} skew angle. Moderate suction are maintained for 90^o and 120^o angle of attack on the entire face A. For 150^o skew angle slightly mild suction is noticed on the upper half of the building while similar suction is prevailing over the major portion face A for 180^o angle of attack.

4.3 Pressure coefficients

The mean pressure coefficient for all surfaces of Type–I cross shaped building are tabulated in the Table 3. The maximum positive mean Cp of face A is observed 0^o wind incidence angle and maximum suction depicted for 60^o angle of attack and the suction is reduced subsequently from 90^o to 180^o angle of attack. Due to symmetry similar Cp values are observed on Face A and Face G just reversing the direction of wind flow. The mean Cp values are positive in nature for face B from 0^o to 90^o angle of attack with maximum (+) 0.914 at 30^o angle of attack as larger surface suffering wind flow directly and for the rest of angle of attack *Cp* values are negative. The mean Cp for all wind incidence angle for face J are negative and Cp values are ranging from (-) 0.443 to (-) 0.503. Unlike 180^o angle of attack mean Cp values for face G and face H are negative in nature for other wind incidence angle. The maximum mean negative Cp of (-) 0.858 is noticed on the face D for 30^o angle of attack while maximum positive mean Cp of (+) 0.917 has been observed on face C for 60^o angle of attack which is due larger frontal surface in the direction of wind flow.

Table 3 Mean pressure Coefficients of all surfaces of building for various wind angles for regular cross shaped building model (Type-I)

Faces / Wind Angles	**0^o**	**30^o**	**60^o**	**90^o**	**120^o**	**150^o**	**180^o**
Face A	0.871	0.222	-0.819	-0.505	-0.462	-0.444	-0.399
Face B	0.511	0.914	0.784	0.540	-0.467	-0.541	-0.402
Face C	0.553	0.783	0.917	0.503	-0.664	-0.542	-0.367
Face D	-0.476	-0.858	0.226	0.869	0.221	-0.807	-0.503
Face E	-0.360	-0.557	-0.665	0.506	0.913	0.784	0.542
Face F	-0.395	-0.550	-0.468	0.540	0.784	0.916	0.503
Face G	-0.396	-0.451	-0.455	-0.515	-0.847	0.227	0.873
Face H	-0.417	-0.395	-0.367	-0.369	-0.554	-0.655	0.506
Face I	-0.374	-0.378	-0.384	-0.405	-0.549	-0.455	0.544
Face J	-0.503	-0.466	-0.448	-0.398	-0.456	-0.443	-0.489
Face K	0.539	-0.466	-0.546	-0.415	-0.390	-0.360	-0.373
Face L	0.500	-0.663	-0.547	-0.371	-0.374	-0.377	-0.420

Table 4 Mean pressure Coefficients of all surfaces of building for various wind angles for angular cross shaped building (Type–II)

Faces / Wind Angles	**0°**	**30°**	**60°**	**90°**	**120°**	**150°**	**180°**
Face A	0.855	0.324	-0.627	-0.543	-0.458	-0.388	-0.357
Face B	0.630	0.919	0.796	0.206	-0.679	-0.494	-0.404
Face C	0.654	0.872	0.896	0.113	-0.797	-0.470	-0.373
Face D	-0.478	-0.311	0.625	0.754	-0.378	-0.623	-0.472
Face E	-0.349	-0.574	-0.276	0.821	0.878	0.762	0.398
Face F	-0.406	-0.542	-0.125	0.702	0.796	0.919	0.335
Face G	-0.372	-0.406	-0.413	-0.455	-0.843	0.325	0.856
Face H	-0.371	-0.347	-0.327	-0.395	-0.578	-0.440	0.645
Face I	-0.346	-0.333	-0.351	-0.427	-0.570	-0.275	0.669
Face J	-0.447	-0.412	-0.368	-0.396	-0.459	-0.422	-0.430
Face K	0.424	-0.547	-0.433	-0.506	-0.399	-0.340	-0.307
Face L	0.234	-0.713	-0.391	-0.448	-0.386	-0.359	-0.355

Table 4 enumerated the details of mean pressure coefficient of building faces for different skew angles ranging from 0^o to 180^o at an interval of 30^o for Type –II building. Similar nature mean face Cp has been observed for face A and face G for different angle of attack in reverse manner with marginal deviation. The negative mean face Cp values have been observed for face J but with lower ranges of magnitude (- 0.368 to -0.459) compared to regular cross shaped building model. Maximum positive mean face Cp value of (+) 0.919 has been noticed on face B for 30^o angle of attack and on face F for 150^o angle of attack due larger frontal surface in particular direction of wind flow. Except 0^o wind incidence angle, for all other wind incidence angles similar negative mean face Cp values are observed for face K and face L but for face H and face I, all face mean Cp values are negative for 0^o to 150^o except 180^o angle of attack. The maximum negative mean face Cp value of (-) 0.847 has been noticed on face G for 120^o angle of attack.

4.4 Variation of pressure coefficient along horizontal line around the building faces

To apprehend peripheral variation of pressure around the building, pressure coefficient at mid height of building model and 30 mm from top edge of building model are presented graphically for various wind incidence angles (Figs. 12-15). For regular cross plan shaped building with 0^o wind angle high magnitude of Cp values more than unity are noticed on all windward faces for both cases at 470 mm from base and mid height of building. Due to symmetry in plan of regular plan shaped building for both cases the distribution of Cp values along the horizontal line are symmetrical for 0^o, 90^o and180^o angle of attack consequently. For other skew angles like 30^o, 60^o, 120^o and 150^o Cp values are positive for the windward faces and negative for rest of the faces (Figs. 12 and 13).

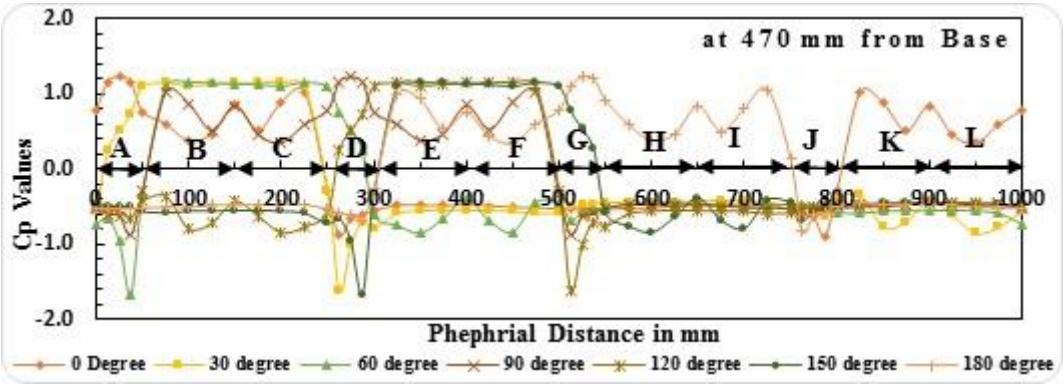

Fig. 12 Variation of Pressure coefficient along horizontal line around building surfaces at distance 470 mm from base for regular cross shaped building (Type–I) for various wind incidence angle

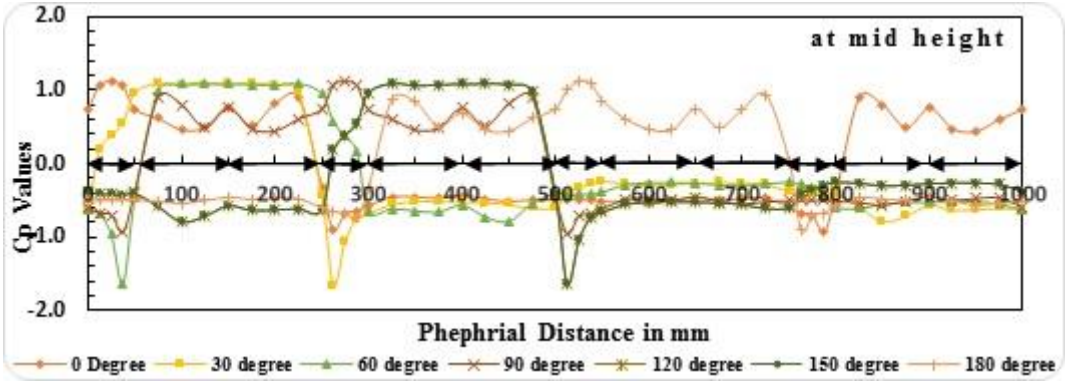

Fig. 13 Variation of pressure coefficient along horizontal line around building surfaces at mid height of regular cross shaped building (Type–I) for various wind incidence angle

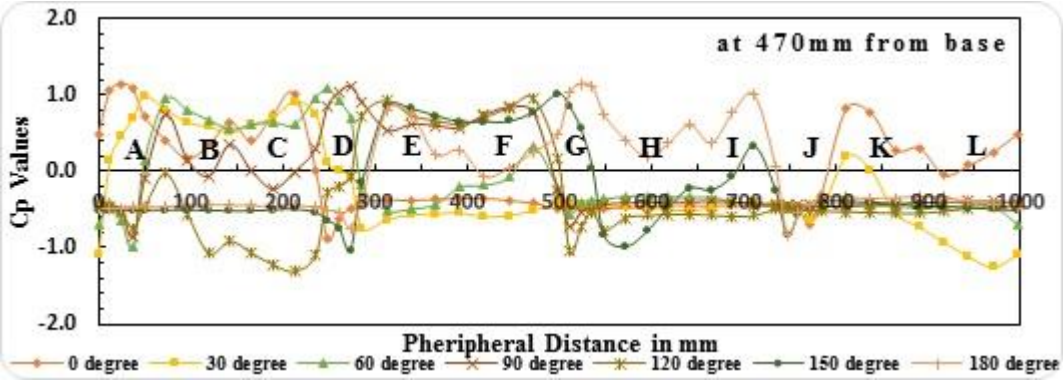

Fig. 14 Variation of Pressure coefficient along horizontal line around building surfaces at height of 470 mm from base for angular cross shaped building (Type–II) for various wind incidence angle

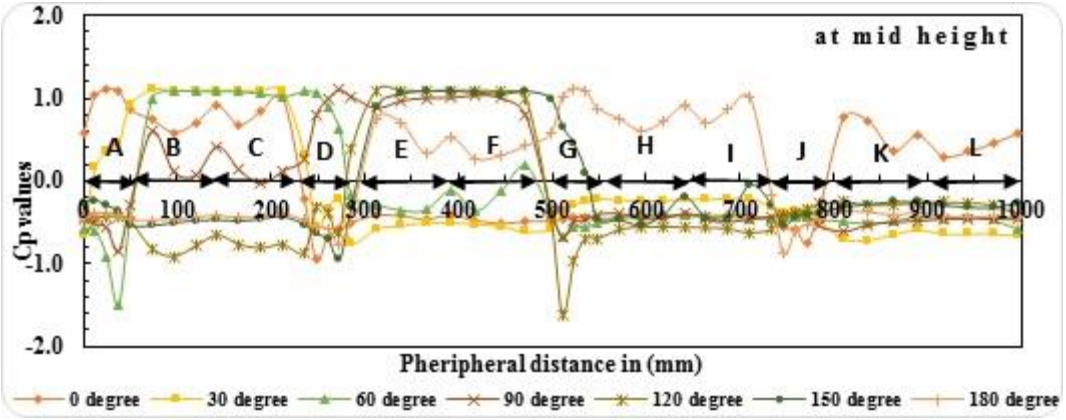

Fig. 15 Variation of Pressure coefficient along horizontal line around building surfaces mid height from base for angular cross shaped building (Type-II) for various wind incidence angle.

For angular cross plan shaped building variation of Cp values along horizontal line is not symmetrical for all angle of attack except for 0^o wind angle. Higher negative Cp values are observed for small region near the edges of owing to separation of wind flow and generation of high vortices particularly for 60^o and 120^o angle of attack at mid height of building. (Figs. 14 and 15).

The variation of pressure coefficients along the horizontal line around the angular cross plan shaped building are presented graphically in the Figs. 16(a)-16(c) for selected wind angles (0^o,90^o and 150^o angle of attack) at three different height (i.e., at 100 mm from base, 250 mm from base and 470 mm from base). Majority of Cp values corresponding to 100 mm from base is smaller than rest of the two cases. Variation of Cp values for 470 mm from base are considered as most vulnerable compared to others due to separation of flow above the building top. Depending upon the shifting of windward faces for various skew angles the positive Cp values are observed to be shifted consequently. For 0^o angle of attack, positive Cp are noticed on face A, face B, face C, face K and face L while face E, face F and Face G are suffering from positive Cp values for 150^o angle attack. For 90^o angle of attack, higher magnitude of Cp values noticed on face D, face E, face F and part of G being on the windward side and but face B and face C possess smaller Cp values due to generation of high vortices in wake region of frontal limb.

4.5 Comparison of Cp along vertical centre line of various faces of the building

Comparison of pressure coefficients along vertical centreline of each faces of angular cross shaped building (Type-II) for wind incidence angle ranging from 0^o to 180^o at an interval of 30^o are represented in Figs. 17(a)-17(l). Positive Cp along the vertical centre line of face A is increasing progressively with height and attain maximum value at around 430 mm from base for 0^o angle of attack (Fig. 17(a)). Unlike 0^o and 30^o angle of attack, negative pressure coefficients are observed for rest of angles of attack for face A. Almost analogous pattern of variation are marked for 30^o and 60^o skew angles for face B and 0^o, 30^o and 60^o skew angles for face C (Figs. 17(b) and 17(c)). However, very marginal range of variation are observed most of the skew angles for Face D. For skew angles ranging from 90^o to 180^o, positive pressure coefficients are noted for face E and face F but lesser negative Cp are observed for rest angle of attacks due to leeward position against wind flow (Fig. 17(e)). Face H and face I mostly exhibited mild negative Cp values for all angle of

attacks except for 180^o angle of attack (Figs. 17(h) and 17(i)). However, negative Cp for all angle of attacks are noticed for Face J. Face K and face L exhibit negative Cp for all angle of attack except for 0^o wind angle (Figs. 17(j)-17(l)).

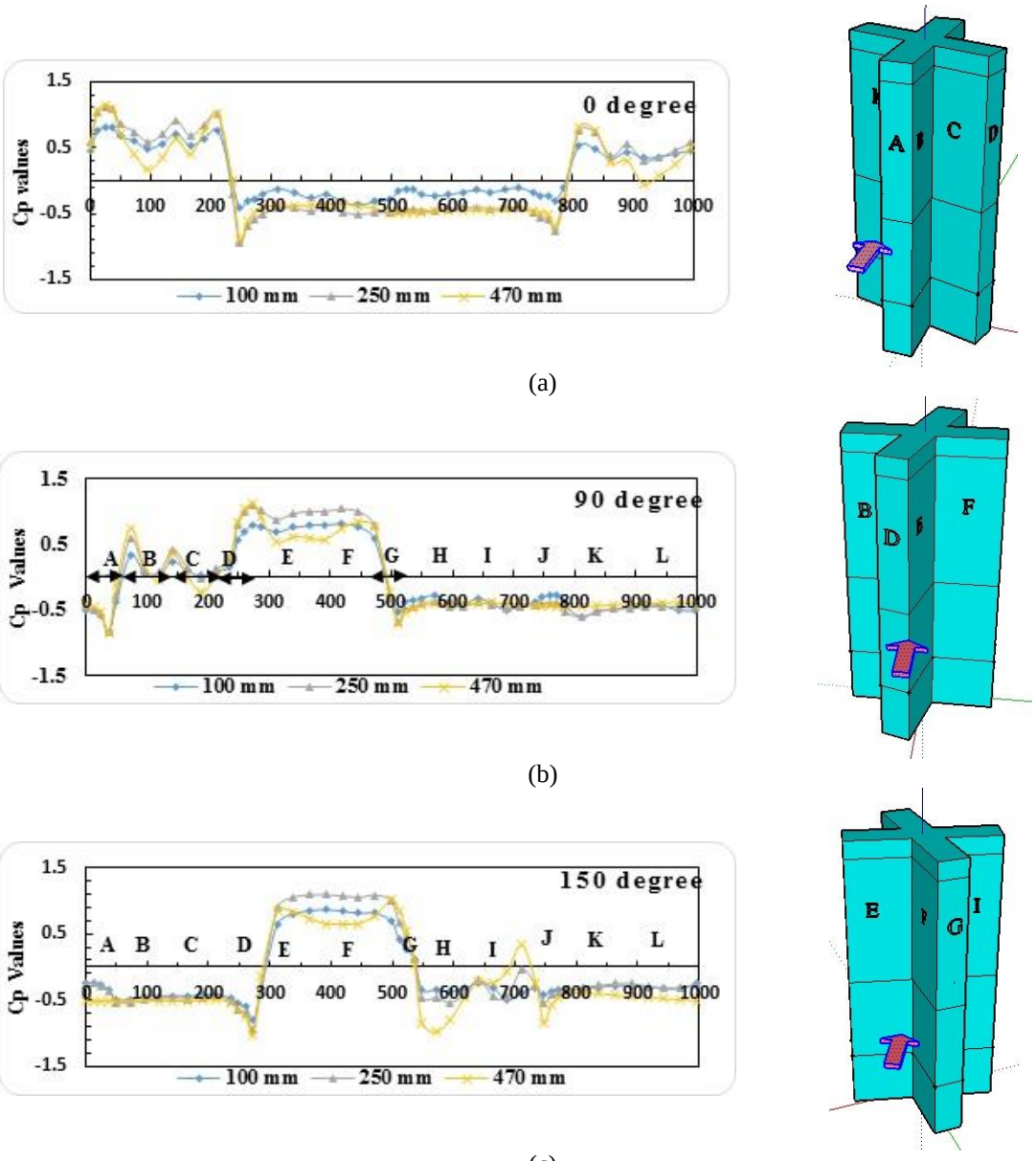

Fig. 16 Comparison of pressure coefficient along different horizontal level (at 100 mm from base, at mid height and 470 mm from base) of angular cross shaped building (Type-II) for various wind incidence angles (a) 0^o , (b) 90^o and (c) 150^o

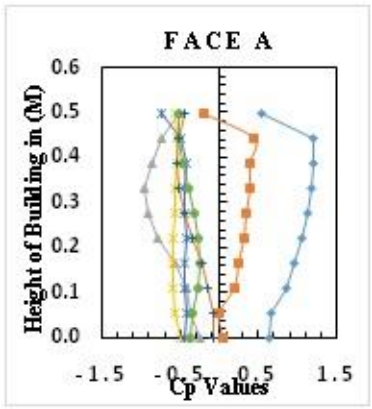

(a)

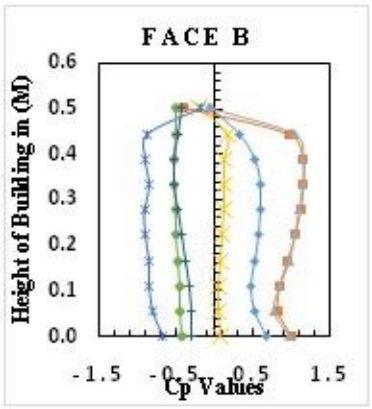

(b)

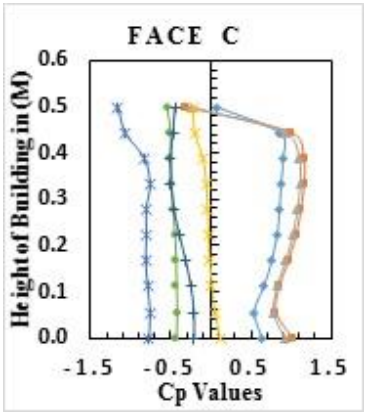

(c)

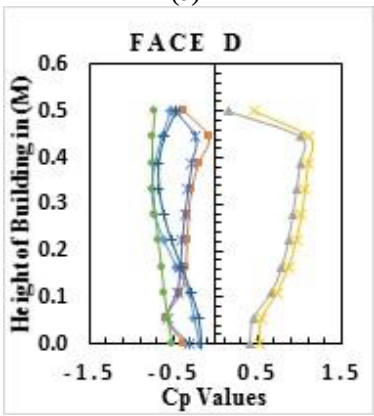

(d)

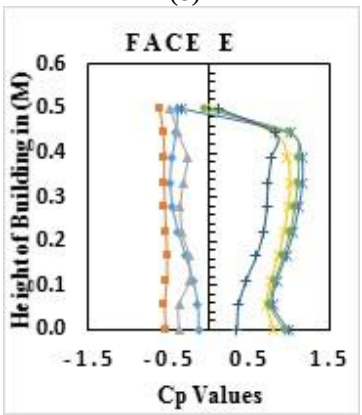

(e)

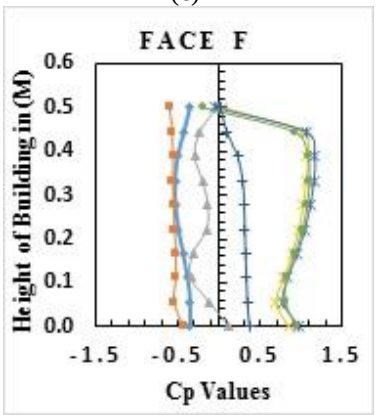

(f)

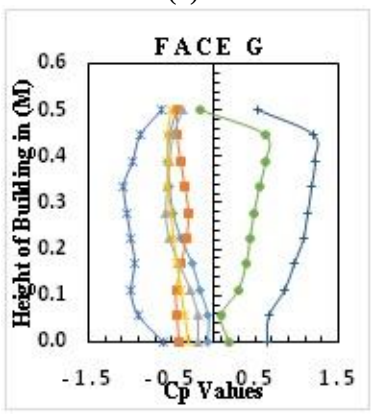

(g)

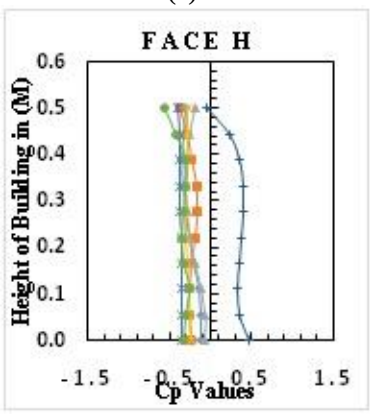

(h)

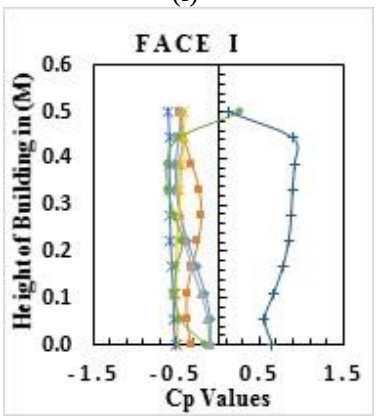

(i)

Continued-

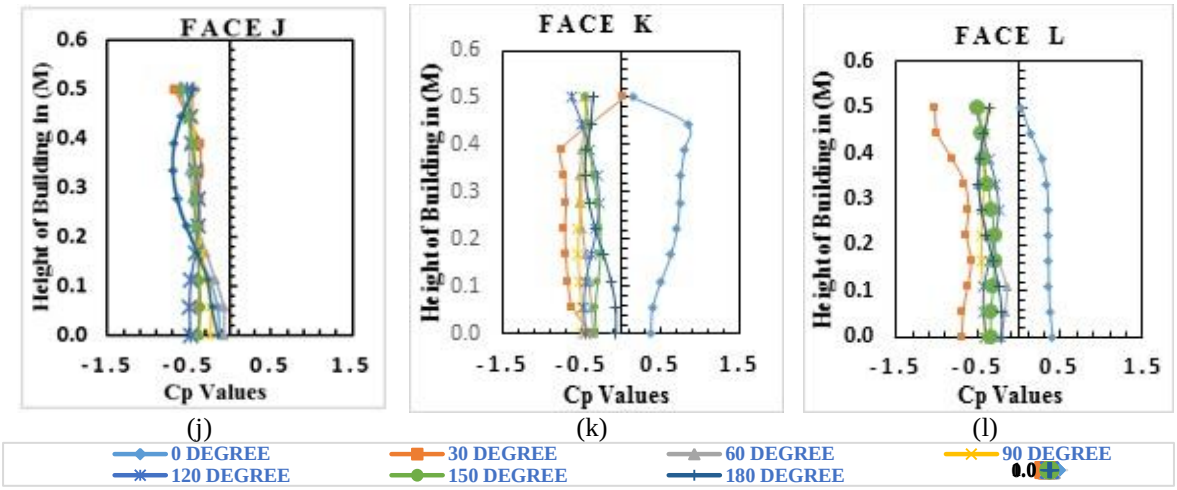

Fig. 17 Comparison of pressure coefficient along vertical centre line of each faces of angular cross shaped building (Type-II) for various wind incidence angles (a) face A, (b) face B, (c) face C, (d) face D, (e) Face E, (f) face F, (g) face G, (h) face H, (i) face I, (j) face J, (k) face K and (l) Face L

4.6 Comparison of pressure coefficients for numerical analysis with experimental results

Generally, k-ε and SST turbulence models are used for the simulation of flow around structures at high Re. To correlate the results obtained from the two models with those from experimental studies in the literature, a comparison is made between present and Chakraborty, Dalui *et al.* (2014a,b) results. Eventually, dimensions and all other parameters related to the wind flow are matched with the numerical studies.

In Table 5, a detailed comparison of mean pressure coefficients obtained from experiment and simulation (both k-ε and SST turbulence models) on each faces of building is made for 0^o wind incidence angle. The mean Cp values for k-ε and SST models nearly matches for all faces. Moreover, a good agreement between numerical and experimental studies is observed except Faces A, C and K. Both numerical results display a higher mean Cp value compared to experimental counterpart, although result obtained from k-ε model have a better agreement with experiment compared to those from SST model.

Further, for regular cross plan shaped building model, simulated pressure coefficients along the vertical centreline (for faces A, B and D) and horizontal centreline around the building at mid depth for 0^o wind incidence angle are compared with experimental as shown in Figs.18(a)-(c) and Fig.19.Negligible variations of pressure coefficient are noticed for k-ε and SST models, respectively, along the vertical centreline for the selected faces of building and also along horizontal centreline around the building. Both numerical results are in good agreement with the experimental results along the vertical centreline of the selected faces but a small discrepancy is observed in Cp values along horizontal line around the building. The discrepancy is attributed to inefficiency or insufficiency of pressure tapping points in capturing the variation of high pressure

at the corner of each faces in wind tunnel test. Moreover, both numerical results over predicted the pressure coefficient values compared to experimental results but deviations are within acceptable limit.

4.7 Force coefficients

Tables 6 and 7 represented the details of along wind and across wind force coefficients for Type – I and Type –II building for various wind incidence angle in x-direction and y-direction (i.e., perpendicular to x-direction) respectively. For regular cross shaped building (Type- I) force coefficient is maximum for 0^o wind incidence angle with magnitude of 1.059 with negligible value in perpendicular direction which matched with values obtained in 180^o just opposite direction due to symmetry of plan shape. The force coefficient in x- direction are reduced significantly for 30^o and 60^o wind incidence angle respectively as shown in Table 5 but progressively increased in y-direction with direction wind flow varies from 0^o to 180^o. For 90^o wind incidence angle force coefficient in y –direction reaches maximum values of 1.063 while negligible value has been noticed in force coefficient value in x- direction.

Table 5 Variation of mean pressure coefficients on different face of building for 0^o wind incidence angle for regular cross plan shaped building model for k-ε model, SST model and experimental results by Chakraborty, Dalui *et al.* (2014a, b)

Faces	Mean Pressure Coefficients			Remarks
	Experimental Results by Chakraborty, Dalui *et al.* (2014a,b)	Numerical Results		
		(k-ε model)	(SST model)	
Face A	0.65	0.871	0.863	All are within acceptable limit.
Face B	0.43	0.511	0.510	
Face C	0.31	0.553	0.549	
Face D	-0.40	-0.476	-0.497	
Face E	-0.38	-0.360	-0.389	
Face F	-0.40	-0.395	-0.422	
Face G	-0.35	-0.395	-0.463	
Face H	-0.40	-0.417	-0.561	
Face I	-0.38	-0.374	-0.527	
Face J	-0.40	-0.503	-0.650	
Face K	0.31	0.539	0.489	
Face L	0.43	0.500	0.489	

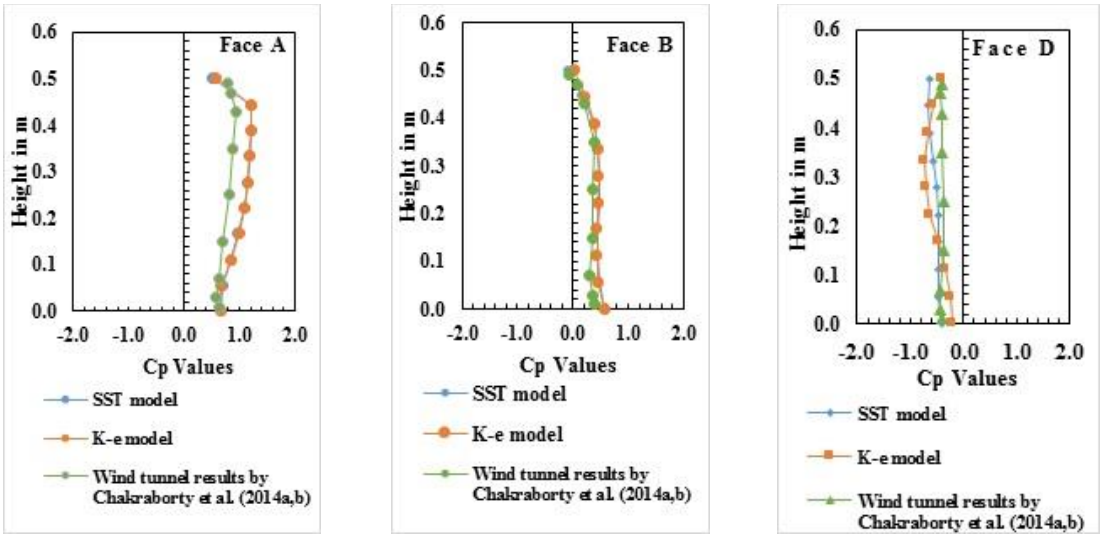

(a) (b) (c)

Fig. 18 Comparison of pressure coefficient along vertical centreline of various faces of building for k-ε model, SST model and experiment results by Chakraborty, Dalui *et al.* (2014a, b) for 0^o wind incidence angle for Type –I building for (a) Face A, (b) Face B and (c) Face D

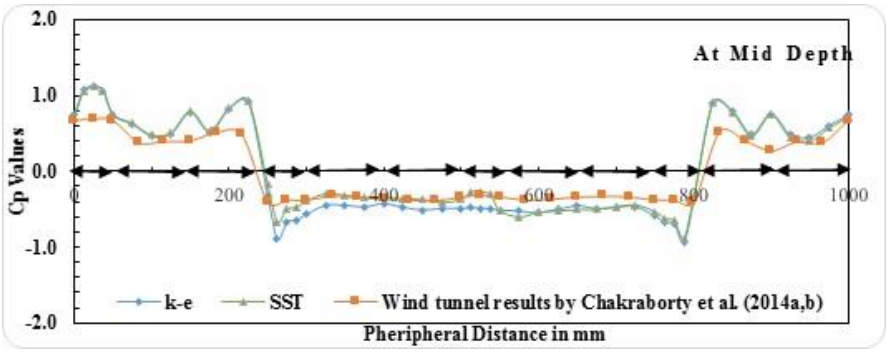

Fig. 19 Comparison of pressure coefficients around the building at mid depth for k-ε model, SST model and experimental results by Chakraborty, Dalui *et al.* (2014a, b) for 0^o wind incidence angle for regular cross plan shaped building

Table 6 Variation of force coefficient with various wind incidence angle for regular cross shaped building model (Type-I)

Wind angles / force coefficient	**0^o**	**30^o**	**60^o**	**90^o**	**120^o**	**150^o**	**180^o**
X-direction (Along the direction of flow)	1.059	0.688	0.513	-0.006 ≅ 0	-0.502	-0.676	-1.058
Y-direction (Across the direction of flow)	0.013 ≅ 0	0.502	0.678	1.063	0.686	0.510	0.007 ≅ 0

Compared to regular cross shaped building model, angular cross shaped building has lesser force coefficient value in x-direction (along wind direction of flow) but considerable increase in force value is noticed for y-direction (across the direction of flow) for 0^o wind angle. Maximum C_f of 0.950 is observed for 180^o angle of attack along the direction of wind flow. For 90^o wind flow, force coefficient in Y-direction is maximum with a magnitude of 1.039 with a considerable C_f in X-direction also noticed. For 30^o and 60^o angle of attack force coefficients in X-direction are marginally reduced compared to regular cross shaped building but in contrast C_f values for Y-direction are amplified slightly.

4.7.1 Comparison of force coefficient of regular and cross plan shaped building model with square plan shaped building model

To better understand effect of variation cross-sectional shape, the regular cross and angular cross plan shaped buildings are finally compared with a square plan shaped building model, having same plan area as that of cross plan shaped model. Thus a square model of 150 mm X 150 mm (plan area = 22500 mm^2) and 500 mm height is being analysed by numerical analysis for similar flow condition. The results are presented in Table 8.

Table 7 Variation of force Coefficient with various wind incidence angle for angular cross shaped building (Type–II)

Wind angles / force coefficient	**0^o**	**30^o**	**60^o**	**90^o**	**120^o**	**150^o**	**180^o**
X-direction (Along the direction of flow)	0.947	0.681	0.410	(-) 0.288	(-) 0.550	(-) 0.688	(-) 0.950
Y-direction (Across the direction of flow)	(-) 0.147	0.462	0.640	1.039	0.774	0.660	0.072

Table 8 Comparison of force coefficient for along wind and across wind direction for regular and angular cross plan shaped building with square plan building model for 0^o wind incidence angle

Type	Plan Area	Force Coefficient		Remarks
		(Along Wind Direction) X-Direction	(Across Wind Direction) Y-Direction	
Angular cross plan shaped building model	22500 mm^2	0.947	(-)0.147	Lesser C_f in along wind direction for angular plan shaped building model.
Regular cross plan shaped building model	22500 mm^2	1.059	0	
Square plan shaped building model	22500 mm^2	1.264	0	

It has been noted that angular plan shaped building possess least along wind force coefficient for 0^o wind incidence angle while square plan shaped model exhibits maximum force coefficient in along wind direction. Thus, it can be concluded that angular plan shaped building model is most efficient compared to the other models. Lesser the force coefficient lesser will be the induced force in whole building. This is due to a fact that the frontal effective area of along wind flow increases considerably for square plan shaped building compared to both cross plan shaped buildings. Further, generation of vortices on the side faces of frontal limb of both cross plan shaped buildings are responsible for the reduction of along wind force coefficients (as shown in Figs. 9(c) and 9(d)) and consequently increase the C_f in across wind direction. On the other hand, regular cross shaped building when symmetrical in plan with respect to direction of flow nullifies the effect of vortices while much prominent across wind effect is noticed for all other unsymmetrical situation. Thus direction of flow and different plan shape of building play major role in developing the magnitude of forces in structures.

5. Conclusions

The present study reveals that wind induced responses differ significantly for regular and angular cross plan shaped buildings. The numerical model, namely 'k-ε model' is mostly used to predict the wind induced responses for both types of building models at flow incidence angles ranging from 0^o to 180^o at interval of 30^o. The notable outcomes of the current study are summarised as follows:

- The effect of mutual interference between faces are prominent on the side of limbs (i.e., faces B and L). However, the side faces of regular rectangular or square plan shaped building are generally subjected to a suction while the side faces of the frontal limb of cross plan shaped building undergo a positive pressure caused by the flow slowing down due to striking on the other surfaces (Face C and K).
- For type II building maximum mean positive pressure coefficients are observed on faces B and F for 30^o and 150^o angle of attack while for type I building maximum mean positive pressure coefficients are noticed on face C for 60^o angle of attack.
- Pressure contour on face A for both Type-I and Type-II buildings for 0^o wind incidence angle more or less similar with regular rectangular or square plan shaped building and maximum positive pressure are observed at around three quarter depth from base. The flow pattern of Type –II building is not symmetrical about vertical axis, slightly shifted towards face B.
- The mean pressure coefficients are negative only for face J for both Type–I and Type–II building in all skew direction of flow.
- For 0^o angle of attack, due to a large flow separation, side faces (like face D, face J etc.) experience a significant suction pressure around the edge for both Type- I and Type II buildings.
- Angular cross plan shaped building, having lowest force coefficient, is more efficient compared to regular and square plan shaped building.
- Further, due to asymmetry in Type-II building, generations of vortices around the side faces of frontal limb are responsible for reduction of along wind force coefficients but increase the in across wind force coefficient for 0^o wind incidence angle.

- Though K-ε and SST models over predicts the pressure coefficient values compared to wind tunnel experiment, the K-ε model results have a better agreement with experimental results.
- For angular plan shaped building the Cp values along horizontal line reveals that top of building (at 470 mm from base) of is quite vulnerable compared to mid height (250 mm from base) and near to the base (100 mm from base).

The results obtained from numerical studies are important for designer to design similar nature of building. As discussed earlier the numerical method is very effective and can be a good weapon to handle such typical irregular plan shaped building and also to predict the critical wind flow direction for a particular plan shape of a building.

References

Amin, J.A. and Ahuja, A.K. (2012), "Wind-induced mean interference effects between two closed spaced buildings", *J. Civil Eng. - KSCE*, **16**(1), 119-131.

Amin, J.A. and Ahuja, A.K. (2013), "Effects of side ratio on wind-induced pressure distribution on Rectangular Buildings", Hindawi Publishing Corporation, *J. Struct*., **2013**, Article ID 176739.

ANSYS, Inc. (2012), ANSYS CFX-Solver Theory Guide, USA, http://www.ansys.com.

AS/NZS: 1170. 2 (2002), Structure design actions, Part – 2: Wind Actions, Australian/ New Zealand Standard; Sydney and Wellington.

ASCE: 7-10 (2010), Minimum design loads for buildings and other structures, Structural Engineering Institute of the American Society of Civil Engineering, Reston.

Bairagi, A.K. and Dalui, S.K. (2014), "Evaluation of interference effects on parallel high-rise buildings for different orientation using CFD", *Proceedings of the 3rd World Conference on Applied Sciences*, Engineering & Technology, Kathmandu, Nepal, September.

Bhattacharyya, B., Dalui, S.K. and Ahuja, A.K. (2014), "Wind induced pressure on 'E' plan shaped tall buildings", *Jordon J. Civil Eng*., **8**(2), 120-134.

Braun, A.L. and Awruch, A.M. (2009), "Aerodynamics and aeroelastic analysis of CAARC standard tall building model using numerical simulation", *J. Wind Eng. Ind. Aerod*., **87**(9-10), 564-581.

Chakraborty, S., Dalui, S.K. and Ahuja, A.K. (2014a), "Wind Load on irregular plan shaped tall building- A case study", *Wind Struct*., **19** (1), 59-73.

Chakraborty, S., Dalui, S.K. and Ahuja, A.K. (2014b), "Experimental and numerical study of surface pressure on'+' plan shape tall building", *Jordon J. Civil Eng*., **8**(3), 251-262.

Dagnew, A.K., Bitsuamalk, G.T. and Merrick, R. (2009), "Computational evaluation of wind pressures on tall buildings", *Proceedings of the 11th American Conference on Wind Engineering*, San Juan, Puerto Rico, June.

Fu, J.Y., Li, Q.S., Wu, J.R., Xiao, Y.Q. and Song, L.L. (2008), " Field measurement of boundary layer wind characteristic and wind induced response of super-tall buildings", *J. Wind Eng. Ind. Aerod*., **96**(8-9),1332-1358.

Gomes, M.G., Rodrigues, A.M. and Mendes, P. (2005), "Experimental and numerical study of wind pressures on irregular-plan shapes", *J. Wind Eng. Ind. Aerod.*, **93**, 741-756.

Gu, M. (2009), "Study on winds and responses on tall building and structures", *Proceedings of the 7th Asia Pacific Conference*, Taipei, Japan, November.

IS: 875(Part –III) (1987), Indian standard code of practice for design loads (other than earthquake) for buildings and structures, Part 3 (wind loads), Bureau of Indian Standards, New Delhi.

Juretic, F. and Kozmar, H. (2013), "Computational modelling of the neutrally stratified atmospheric boundary layer flow using the standard k–ε turbulence mode", *J. Wind Eng. Ind. Aerod.*, **115**, 112-120.

Kar, R. and Dalui, S.K. (2015), "Wind interference effect on an octagonal plan shaped tall building due to

square plan shaped tall buildings", *Int. J. Adv. Struct. Eng*., **8**(1), 73-86.
Kheyari, P. and Dalui, S.K. (2014), "Interference effects on tall building under wind excitation for various incidence angle using CFD code", *Proceedings of the 3rd World Conference On Applied Sciences*, Engineering & Technology, Kathmandu, Nepal, September.
Kushal, T., Ahuja, A.K. and Chakrabarti, A. (2013), "An experimental Investigation of Wind Pressure Developed in Tall Buildings for different plan Shape", *Int. J. Innovative Res. Studies*, **2**(6), 606-614.
Lam, K.M., Wong, S.Y. and To, A.P. (2009), "Dynamic wind loading of H-shaped tall buildings", *Proceedings of the* 7th Asia-Pacific Conference on Wind Engineering, Taipei, Japan, November.
Mendis, P., Ngo, T., Haritos, N., Hira, A., Samali, B. and Cheung, J. (2007), "Wind Loading on tall buildings", EJSE Special Issue: Loading on Structures (**2007**), 41-54.
Mukherjee, S., Chakraborty, S., Dalui, S.K. and Ahuja, A.K. (2014), "Wind Induced pressure on 'Y' plan shape tall building", *Wind Struct*., **19**(5), 523-540.
Raj, R. and Ahuja, A.K. (2013), "Wind Loads on cross shape tall buildings", *J. Academia Ind. Res*. (JAIR), **2**(2), July.
Revuz J., Hargreaves, D.M. and Owen, J.S. (2012), "On the domain size of steady state CFD modelling of tall building", *Wind Struct*., **15**(4), 313-329.
Sevalia, J.K., Desai, A.K. and Vasanwala, S.A. (2012), "Effect of geometric plan configuration of tall building on wind force coefficient using CFD", *Int. J. Adv. Eng. Res. Studies*, **1**(2), 127-130.
Tanaka, H., Tamura, Y., Ohtake, K., Nakai, M. and Kim, Y.C. (2012), "Experimental investigation of aerodynamic forces and wind pressures acting on tall buildings with various unconventional configurations", *J. Wind Eng. Ind. Aerod*., **107-108**, 179-191.
Verma, S.K., Ahuja, A.K. and Pandey, A.D. (2013), "Effects of wind incidence angle on wind pressure distribution on square pan tall buildings", J. Academic Ind. Res., **1**(12), 747-752.
Zhou, Y., Kijewski, T. and Kareem, A. (2002), "Along-wind load effects on tall buildings: Comparative study of major international codes and standards", *J. Struct. Eng. - ASCE*, **128** (6), 788-796

AD